# **PROCEEDINGS OF SPIE**

SPIEDigitalLibrary.org/conference-proceedings-of-spie

# Deep UV microscopy of prostate cancer tissue

Soltani, Soheil, Ojaghi, Ashkan, Kludze, Atsutse, Robles, Francisco

Soheil Soltani, Ashkan Ojaghi, Atsutse Kludze, Francisco E. Robles, "Deep UV microscopy of prostate cancer tissue," Proc. SPIE 11243, Imaging, Manipulation, and Analysis of Biomolecules, Cells, and Tissues XVIII, 1124317 (17 February 2020); doi: 10.1117/12.2546200



Event: SPIE BiOS, 2020, San Francisco, California, United States

# Deep UV Microcopy of prostate cancer tissue

Soheil Soltani\*a, Ashkan Ojaghi a, Atsutse Kludze b, Francisco E Robles a aWallace H. Coulter Dept. of Biomedical Engineering Georgia Institute of Technology and Emory University, 313 Ferst Dr. NW, Atlanta, GA 30332, USA bS.U.R.E program, Georgia Institute of Technology ,313 Ferst Dr. NW, Atlanta, GA 30332, USA

#### **ABSTRACT**

Correctly diagnosing and staging prostate cancer continues to be a significant clinical challenge. Currently, the standard of care consists of a pathologist's visual assessment of hematoxylin-and-eosin-stained (H&E) histological sections, and designation of a Gleason score based on the top two most common patterns. However, this process is subjective and thus prone to error. Further, lack of standard protocols for staining, makes quantitative analysis of stained tissues difficult. Therefore, there is a significant need to develop new quantitative methods that can provide robust, objective, and accurate information of the aggressiveness and stage of prostate cancer.

In this work, we seek to address this challenge using multi-spectral deep-UV microscopy of unstained tissue sections. This method yields valuable insight into the aggressiveness and stage of the disease due to its subcellular spatial resolution and high sensitivity to many endogenous biomolecules, including nucleic acid and proteins.

In our approach we use a simple and cost effective wide-field imaging configuration with sequential illumination at multiple wavelengths ranging from 220 nm to 450 nm. Spectral signatures are analyzed in conjunction with the morphology using a geometrical representation of principal component analysis and principles of mathematical morphology. Our results reveal distinct morphological and molecular alterations in the tissue as cancer becomes more aggressive. In this presentation we will detail the design of the multispectral, deep UV microscope; describe our quantitative image analysis; and show preliminary results.

Keywords: Microscopy, Ultra-Violet microscopy, tissue imaging, multi-spectral imaging

# 1. INTRODUCTION

Prostate cancer is the most commonly diagnosed non-skin cancer and is the second leading cause of death in the United State[1]. Therefore, it is crucial to determine the appropriate and the most effective treatment plan to improve the survival rate of patients with prostate cancer. One of the most critical factors in evaluating different treatment options is the stage of prostate cancer and its aggressiveness. Any variations and inaccuracy in determining the stage of prostate cancer might result in ineffective treatment that might have serious consequences for patients. Current standard method for determining stage of prostate cancer is evaluation of histological hematoxylin-and-eosin-stained (H&E) slices of biopsy samples and assessment of the two most dominant patterns based on the "Gleason grading" system [2-4]. Even though the Gleason grade is the most commonly used method for staging prostate cancer, it has fundamental limitations. Assessing Gleason grade is a qualitative and thus subject to human error and decision variability [5, 6]. Therefore, evaluating the stage of prostate cancer based on this qualitative and subjective system does not always lead to the most effective treatment option for all the patients.

In an effort to provide robust quantitative information that could improve prostate cancer diagnosis and staging, we have developed a label-free multispectral deep ultraviolet (UV) microscopy technique to study unstained tissue sections. Using the unique endogenous molecular signatures in the deep UV region of spectrum, it is possible to identify the spatial resolution of many important endogenous biomolecules with subcellular resolution [7, 8]. We will show that deep UV microscopy enables us to quantitatively analyze prostate cancer tissue slides.

Imaging, Manipulation, and Analysis of Biomolecules, Cells, and Tissues XVIII, edited by Daniel L. Farkas, Attila Tarnok, Proc. of SPIE Vol. 11243, 1124317 ⋅ © 2020 SPIE ⋅ CCC code: 1605-7422/20/\$21 ⋅ doi: 10.1117/12.2546200

# 2. SYSTEM DESIGN

Our multi-spectral UV imaging scheme uses a plasma-driven broadband light source (Energetiq, EQ-99X) that provides a continuous spectrum from 200 nm to around 2 µm. Previously we have shown that many important biomolecules have unique signatures in deep UV region of spectrum from 220 nm to 400nm. Therefore, we use select wavelengths that contain dominant spectral absorption features in this range from molecules such as protein, nucleic acid, etc. Here we specifically chose 4 wavelengths: 220nm,255nm, 280 nm and 300 nm. For each acquisition we selected one wavelength using a band-pass filter with a bandwidth of 10 nm. The output beam from the UV source is used to illuminate the sample using an off-axis parabolic mirror. The transmitted light is collected through a Thorlabs (LMU-40X-UVB) UV objective and is relayed on a UV camera (PCO. Ultraviolet) using a biconvex lens (f=150 mm). A schematic of imaging set up is shown in Fig.1.

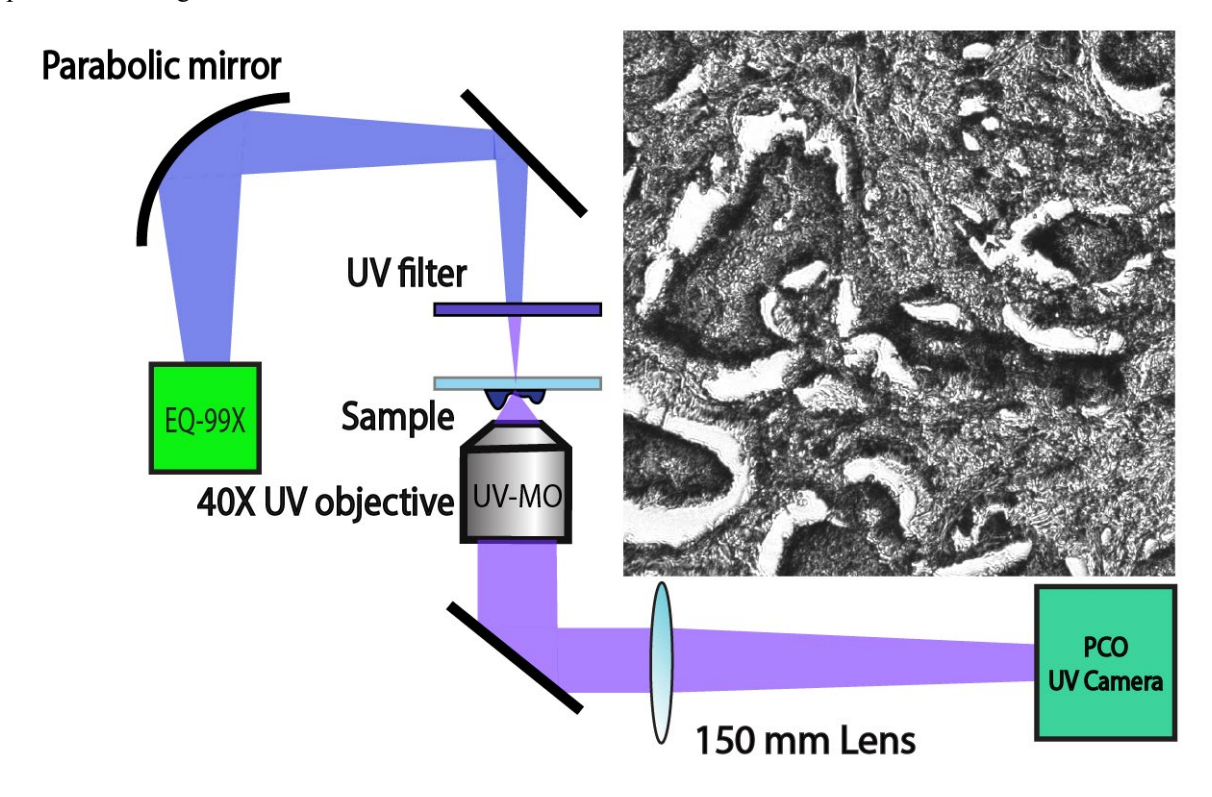


Figure.1 Schematic of the testing set up

For each area of interest, a multispectral data cube is taken at four different wavelengths by rotating a filter wheel to choose the corresponding wavelength. (220,255,280 and 300 nm). For each acquisition we have varied the integration time so that the maximum pixel value is close to saturation and therefore maximum dynamic range is utilized. The acquisition times are around 320, 11, 3.8 and 5.3 ms for 220 nm, 255nm , 280 nm and 300nm respectively. The difference in integration time for the four wavelengths arises from variations in spectral intensity of the light source and different absorption levels of the tissue. The field of view for each acquisition is  $\sim 200x200~\mu m$  and resolution is  $\sim 250~nm$ .

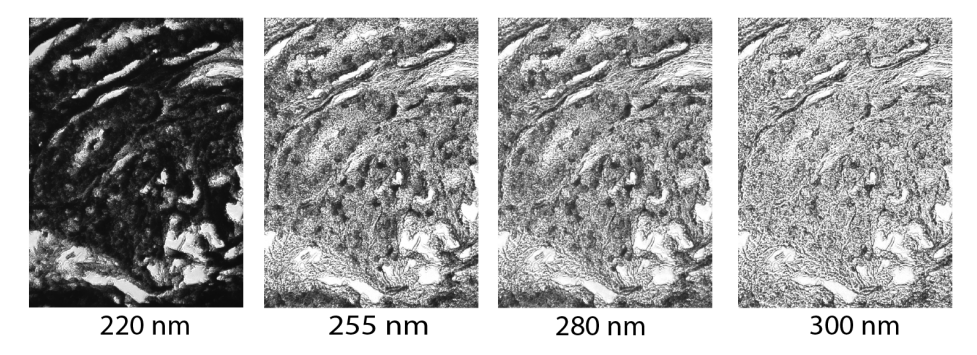


Figure.2 Deep UV images taken at different wavelengths.

# 3. ANALYSIS AND DISCUSSION

In order to separate data points based on spectral similarities, we use a geometrical representation of principal component analysis. To this end, first we calculate the principal components from select regions of interest that contain representative structures of prostate tissue. Surprisingly the calculated principal components were very similar to the expected scattering dependence of tissue, and absorption spectra of nucleic acid and proteins.

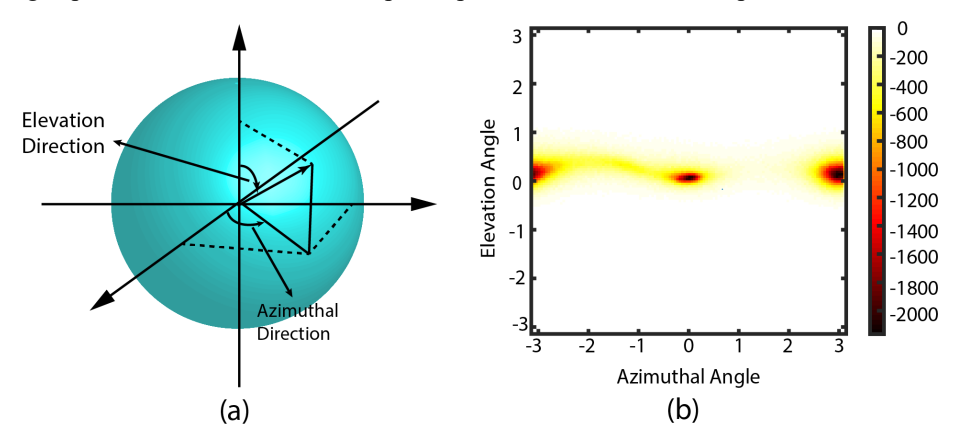


Figure.3 (a) Schematic of Elevation and azimuthal direction used in our method (b) An example of the spherical coordinate histograms used in our study

Next the top 3 principal component projections are described in spherical coordinates, which represents the continuum of molecular composition where the angles (azimuth and elevation angles) fully describe the molecular information while the radius is a measure of the relative concentration [9]. We have shown a schematic of the spherical coordinate representations as well as an example of a histogram in elevation-azimuthal domain in fig.3. The projection of the data points on spherical coordinates creates a histogram that has different features which shows some average variability based on cancer grade. We used 120 regions from Gleason grade raging from 3 to 5 to create a histogram for each stage and compared them to each other. The results show that the cumulative histograms for each stage of prostate cancer has a slightly different distribution, which could be used as a quantitative surrogate biomarker for prostate cancer staging. This information in combination with the structure could also provide additional information that can be used to better differentiate between Gleason grades [10].

# 4. CONCLUSION

In conclusion, we have developed a multi spectral deep UV microscopy technique that uses distinct spectral features of biomolecules in the UV spectrum to provide unique quantitative molecular and structural information of histological samples. We have used our microscopy system to study prostate histological tissue slides. We have used geometrical representation of principal component analysis to separate and categorize regions with Gleason Grades 3, 4 and 5. Since our system is fast, cost-effective and easy to use, it provides a powerful means to study, prostate cancer with high resolution and can potentially help in better staging and diagnosis this disease.

### 5. ACKNOWLEDGMENTS

We gratefully acknowledge Dr. Adeboye Osunkoya for lending his expertise in histopathologoy, and the funding sources for this work: National Science Foundation (NSF CBET CAREER 1752011); Burroughs Welcome Fund (CASI BWF1014540); Galloway Foundation and Integrated Cancer Research Center, Georgia Institute of Technology.

### 6. REFERENCES

- 1. O. W. Brawley, "Prostate cancer epidemiology in the United States," World Journal of Urology **30**, 195-200 (2012).
- 2. J. Gordetsky and J. Epstein, "Grading of prostatic adenocarcinoma: current state and prognostic implications," Diagnostic Pathology **11**, 25 (2016).
- 3. P. A. Humphrey, "Gleason grading and prognostic factors in carcinoma of the prostate," Modern Pathology **17**, 292-306 (2004).
- 4. F. Brimo, R. Montironi, L. Egevad, A. Erbersdobler, D. W. Lin, J. B. Nelson, M. A. Rubin, T. van der Kwast, M. Amin, and J. I. Epstein, "Contemporary Grading for Prostate Cancer: Implications for Patient Care," European Urology **63**, 892-901 (2013).
- 5. M. B. Culp, I. Soerjomataram, J. A. Efstathiou, F. Bray, and A. Jemal, "Recent Global Patterns in Prostate Cancer Incidence and Mortality Rates," European Urology 77, 38-52 (2020).
- 6. R. L. Siegel, K. D. Miller, and A. Jemal, "Cancer statistics, 2019," CA: A Cancer Journal for Clinicians **69**, 7-34 (2019).
- 7. S. Soltani, A. Ojaghi, and F. E. Robles, "Deep UV dispersion and absorption spectroscopy of biomolecules," Biomed. Opt. Express **10**, 487-499 (2019).
- 8. A. Ojaghi, M. E. Fay, W. A. Lam, and F. E. Robles, "Ultraviolet Hyperspectral Interferometric Microscopy," Scientific Reports **8**, 9913 (2018).
- 9. F. E. Robles, S. Deb, J. W. Wilson, C. S. Gainey, M. A. Selim, P. J. Mosca, D. S. Tyler, M. C. Fischer, and W. S. Warren, "Pump-probe imaging of pigmented cutaneous melanoma primary lesions gives insight into metastatic potential," Biomed. Opt. Express 6, 3631-3645 (2015).
- 10. F. Robles, J. Wilson, and W. Warren, "Quantifying melanin spatial distribution using pump-probe microscopy and a 2-D morphological autocorrelation transformation for melanoma diagnosis," Journal of Biomedical Optics **18**, 120502 (2013).